

## Perspective Assessment of COX-1 and COX-2 Selectivity of Nonsteroidal Anti-Inflammatory Drugs from Clinical Practice: Use of Genetic Function Approximation

Ajit P. Zambre,<sup>†</sup> Ashok L. Ganure,<sup>‡</sup> Devanand B. Shinde,<sup>‡</sup> and Vithal M. Kulkarni<sup>\*†</sup>

Department of Pharmaceutical Chemistry, Bharati Vidyapeeth University, Poona College of Pharmacy, Pune 411 038, India, and Department of Chemical Technology, Dr. Babasaheb Ambedkar Marathwada University, Aurangabad 431 004, India

Received October 10, 2006

The beneficial action of nonsteroidal anti-inflammatory drugs (NSAIDs) is associated with the inhibition of cyclooxygenase-2 (COX-2), whereas their harmful side effects are associated with the inhibition of COX-1. In order to understand a meaningful comparison of both classical NSAIDs and newer COX-2 drugs, a series of molecules from varied classes of COX-2 inhibitors was studied by the application of three-dimensional quantitative structure–activity relationships (3D-QSAR) using molecular descriptors obtained by genetic function approximation. The features responsible for the dual inhibition of COX-1 and COX-2 and the selective inhibition of COX-2 with factors contributing to the maintenance of optimum selectivity were identified. The QSAR models revealed the importance of thermodynamic, electronic, structural, and molecular shape analysis parameters, which can reasonably modulate the selectivity pattern to avoid unsolicited side effects. An improved understanding to rationalize the COX-1 and COX-2 binding profiles could be gained to develop safe drug design methods.

### INTRODUCTION

Inflammation is a complicated response involving several cell types and many putative mediators and modulators.<sup>1</sup> It is well-documented that nonsteroidal anti-inflammatory drugs (NSAIDs) exert anti-inflammatory and analgesic effects through the inhibition of prostaglandin (PG) synthesis, by blocking cyclooxygenase (COX) activity.<sup>2</sup> Two isoforms of the COX enzyme, COX-1 and COX-2, with their functional roles in the maintenance of normal homeostasis and induction of inflammation at inflammatory sites, respectively, were identified early in the past decade.<sup>3,4</sup> Traditional NSAIDs, namely, indomethacin, ketoprofen, and ketorolac, being nonselective for these two different isoforms, block the overall production of PGs, which disrupts the beneficial PG-regulated process leading to life-threatening ulcerogenic side effects, thereby limiting their therapeutic potential.<sup>5</sup> In fact, diclofenac, a nonselective inhibitor, has a stronger affinity for COX-2 than COX-1.<sup>6</sup> In order to speed up drug development for safer NSAIDs, the discovery of the second isoform (COX-2) has taken a new turn, to have exclusive control over inflammatory processes, leaving other tissues unharmed even during chronic treatment. This has been truly supported and accepted worldwide by the introduction of selective COX-2 inhibitors, celecoxib (Pfizer)<sup>7</sup> and rofecoxib (Merck)<sup>8</sup> followed by valdecoxib,<sup>9</sup> paracoxib Na,<sup>10</sup> and etoricoxib<sup>11</sup> as current generation drugs. However, the worldwide withdrawal of rofecoxib because of its increased risk of cardiovascular events made an issue of the importance

of targeting selectivity for COX-2 and/or COX-1.<sup>12</sup> New selective COX-2 inhibitors continue to emerge at an unprecedented speed, many of which are variations of tricyclic or classical NSAIDs. Extensive efforts were made to establish a correlation with structural parameters and biological activity on diverse series of compounds using three-dimensional quantitative structure–activity relationship (3D-QSAR) studies.<sup>13–15</sup>

Though the crystal structure of bovine COX-1, murine COX-2, and human COX-2 enzymes with or without ligands are solved, the de novo design or optimization of COX-2 selectivity of inhibitors is not an easy task and may also be concerned with the physicochemical and kinetic factors hidden in the X-ray crystal structure and the flexibility of the COX-1 and COX-2 active sites.<sup>16</sup> In such cases, generating 3D-QSAR models using various physicochemical descriptors can yield information to understand the factors responsible for optimum biological activity against two isoforms of COX. Our strategy follows the methodology used previously to generate successful 3D-QSAR models for antifungal, antibacterial, antiHIV-1, antidiabetic, and anti-tubercular agents.<sup>17–21</sup>

In order to deduce the correlation between the structural and biological activities of the present series of molecules containing classical NSAIDs and new COX-2 inhibitors, genetic function approximation (GFA), developed by Rogers,<sup>22,23</sup> has been used to generate different 3D-QSAR models from various descriptors available within the Cerius2 molecular modeling software.<sup>24</sup> GFA involves the combination of Friedman's multivariate adaptive regression splines algorithm and Holland's genetic algorithm to evolve a population of equations that best fit the training set data.<sup>22–23,25–28</sup>

\* Corresponding author phone: +91 20 2543 7237; fax: +91 20 2543 9383; e-mail: vivivips5@gmail.com.

<sup>†</sup> Bharati Vidyapeeth University.

<sup>‡</sup> Dr. Babasaheb Ambedkar Marathwada University.

This is done as follows: (a) An initial population of equations is generated by a random choice of descriptors. The fitness of each equation is scored by lack-of-fit (LOF) measure

$$\text{LOF} = \frac{\text{LSE}}{\{1 - (c + d \times p)/m\}^2}$$

where, LSE is the least-square error,  $c$  is the number of basis functions in the models,  $d$  is the smoothing parameter which controls the number of terms in the equation,  $p$  is the number of features contained in all terms of the models, and  $m$  is the number of compounds in the training set. (b) Pairs from the population of equations are chosen at random, and "crossovers" are performed, and progeny equations are generated. (c) The fitness of each progeny equation is assessed by the LOF measure. (d) If the fitness of the new progeny equation is better, then it is preserved. The model with a proper balance of all statistical terms will be used to explain the variance in the biological activity.

The combination of the robust statistical technique GFA with the use of different types of descriptors would result in better prediction of the biological activity for COX-2 enzyme inhibitors as safer anti-inflammatory agents. In this paper, we present 3D-QSAR models for known NSAIDs available in clinics using different molecular descriptors with the GFA algorithm to find the features responsible for activity against COX-1 and COX-2 and the factors responsible for the selective inhibition of COX-2. A total of 33 parameters were calculated and were correlated with the biological activity.

## MATERIALS AND METHODS

**Biological Data.** A data set of 32 known NSAIDs in clinical practice was used for which  $\text{IC}_{50}$  values for both COX-1 and COX-2 inhibition and the selectivity index (SI) ( $\text{COX-2}/\text{COX-1}$ ) were reported against a human whole blood assay and a William Harvey modified assay. The logarithm of measured inhibitory activity against respective enzymes COX-1 and COX-2 was used as dependent variable, thus correlating the data linear to the free energy change. It is imperative to evaluate the predictivity of the 3D-QSAR models generated. The molecules were divided into training and test sets. Selection of the training set and the test set molecules was done by considering the fact that test set molecules represent a range of biological activities similar to that of the training set. Thus, the test set is a true representative of the training set. The structures of the training set and test set molecules are given in Tables 1 and 2, respectively.

**Molecular Modeling.** All molecular modeling studies were carried out using Cerius2 (version 3.5) on a Pentium IV workstation.<sup>28</sup> The structures of molecules were constructed using the 3D sketcher available in the BUILD module with Universal Force Field 1.02, and the partial atomic charges were calculated using the charge equilibration approach.<sup>29</sup> All of the molecules were subsequently minimized by a conjugate gradient algorithm to achieve a root-mean-square deviation of 0.001 kcal/mol Å and used in the present study.

**Computation of Molecular Descriptors.** The Cerius2 QSAR+ module provides a wide variety of molecular descriptors containing 27 descriptors as a default data set.

In the present study, 33 various types of molecular descriptors were calculated for each molecule in the study table, which includes electronic, thermodynamic, structural, conformational, spatial, and molecular shape analysis (MSA) descriptors as shown in Table 3. In addition to the default set, MSA descriptors were calculated using the MSA module within Cerius2.<sup>30</sup> A conformational analysis on all of the molecules was performed by using a random sampling search option with the number of conformers limited to 150 and a relative cutoff of 10 kcal. The lowest-energy conformer of the most active molecule was selected as a shape reference, and MSA descriptors were calculated.<sup>30</sup> Tenoxicam, DuP-697, and rofecoxib were used as shape references for COX-1 activity, COX-2 activity, and selectivity analysis, respectively.

**QSAR and GFA.** QSAR analysis is an area of computational research, which builds models of biological activity using physicochemical properties of a series of compounds. The underlying assumption is that the variations of biological activity within a series can be correlated with changes in measured or computed molecular features of the molecules. In the present study, QSAR model generation was performed by the GFA technique. Application of the GFA algorithm allows the construction of high-quality predictive models and makes available additional information not provided by standard regression techniques, even for data sets with many features. GFA was performed using 100 000 crossovers, a smoothness value of 1.00, and other default settings for each combination. GFA was asked to consider a predetermined number of terms in the equation depending upon the number of molecules in the training set. A population of 100 equations was generated in each run by using a set of 33 descriptors and linear basis functions. The generated equations were evolved by repeating the GFA runs to check the stability of GFA models indicating convergence of the calculations. The number of terms in the equation was thus fixed to four as analyzed statistically to obtain the best model. The final set of GFA models was evaluated on the following basis: (a) the LOF measure, (b) variable terms in the equation, and (c) the internal and external predictive ability of the equation. Cross-validated  $r^2$  ( $r^2_{\text{cv}}$ ) and randomized cross-validated  $r^2$  values were calculated using the cross-validated test option in the statistical tools supported in Cerius2.

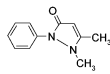
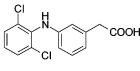
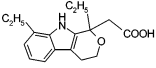
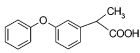
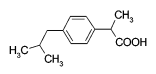
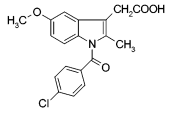
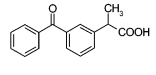
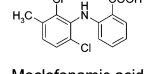
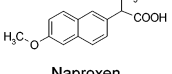
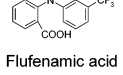
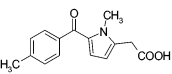
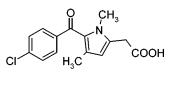
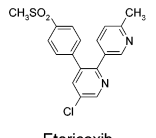
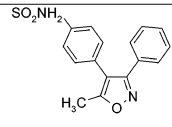
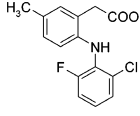
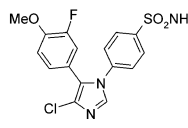
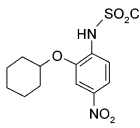
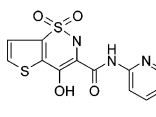
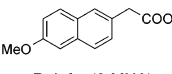
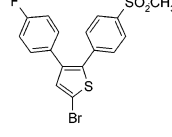
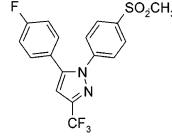
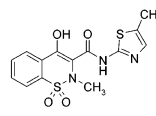
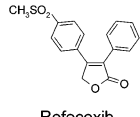
The predictive  $r^2$  was based only on molecules not included in the training set and is defined as

$$r^2_{\text{pred}} = \frac{(\text{SD} - \text{PRESS})}{\text{SD}}$$

where SD is the sum of the squared deviations between the biological activity of molecules in the test set and the mean biological activity of the training set molecules and PRESS is the sum of the squared deviations between predicted and actual activity values for every molecule in the test set. Like  $r^2_{\text{cv}}$ , predictive  $r^2$  can assume a negative value, reflecting a complete lack of predictive ability of the training set for the molecules included in the test set.<sup>31,32</sup> Observed and predicted biological activities of test molecules along with residuals have been presented in Table 6.

**Randomization Tests and Full Cross Validation Test.** To determine the model's reliability and significance, the randomization procedure was performed at 95% (19 trials)

**Table 1.** Structures of Molecules Belonging to the Training Set

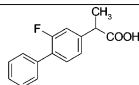
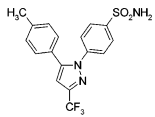
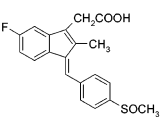
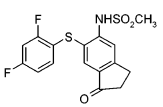
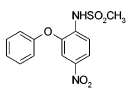
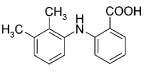
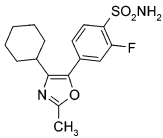
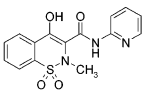
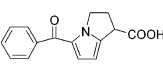
Sr. No.	Molecule	-log IC <sub>50</sub> (COX-1)	-log IC <sub>50</sub> (COX-2)	Selectivity Index (SI) (COX-2/COX-1)
1.	 Phenazone	1.26	1.07	0.849
2.	 Diclofenac	4.12	4.70	1.140
3.	 Etodolac	1.20	3.03	2.525
4.	 Fenoprofen	2.47	2.23	0.902
5.	 Ibuprofen	2.12	1.69	0.797
6.	 Indomethacin	1.72	2.92	1.697
7.	 Ketoprofen	4.33	3.62	0.836
8.	 Meclofenamic acid	3.66	3.70	1.010
9.	 Naproxen	2.03	1.46	0.719
10.	 Flufenamic acid	1.60	1.96	1.225
11.	 Tolmetin	3.46	2.89	0.835
12.	 Zomiperac	3.37	4.02	1.192
13.	 Etoricoxib	3.935	5.958	1.514
14.	 Valdocoxib	4.583	6.060	1.322
15.	 Lumaricoxib	5.494	6.795	1.236
16.	 Cimicoxib	3.903	7.180	1.839
17.	 NS-398	5.317	6.327	1.189
18.	 Tenoxicam	5.638	4.847	0.859
19.	 Relafen(6-MNA)	3.826	3.638	0.950
20.	 DuP-697	5.280	7.221	1.218
21.	 SC-58125	4.522	5.647	1.248
22.	 Meloxicam	2.24	3.64	1.625
23.	 Rofecoxib	1.20	3.51	2.925

and 98% (49 trials) confidence levels. The randomization was done by repeatedly permuting the dependent variable set (i.e., the mean activity data). If the score of the original QSAR model proved better than those from the permuted data sets, the model would be considered statistically significant and better than those obtained from the permuted data. The results of 19 and 49 trials of randomization tests are shown in Table 4. The correlation coefficient,  $r^2$ , for the nonrandom QSAR model was 0.775, significantly better than

those obtained from randomized data ( $r^2 = 0.194$  and  $0.163$  for 19 and 49 trials, respectively). None of the 19 and 49 permuted sets produced  $r^2$  comparable with 0.775; hence, the value obtained for the original GFA model for 32 molecules could be considered significantly different from zero with  $p < 0.05$ .

A full cross-validation has also been done for one of the best GFA models from COX-1 and COX-2 activity and selectivity index data sets. Standard cross-validation in GFA

**Table 2.** Structures of Molecules in the Test Set

Sr. No.	Molecule	-log IC <sub>50</sub> (COX-1)	-log IC <sub>50</sub> (COX-2)	Selectivity Index (SI) (COX-2/COX-1)
24.	 Flurbiprofen	4.12	3.11	0.754
25.	 Celecoxib	2.92	3.47	1.188
26.	 Sulindac	4.89	3.89	0.795
27.	 L-745337	1.00	2.89	2.89
28.	 Nimesulide	2.00	3.41	1.705
29.	 Mefenamate	1.60	2.89	1.806
30.	 Tiracoxib (JTE-522)	4.000	7.070	1.767
31.	 Piroxicam	2.62	3.77	1.438
32.	 Ketorolac	6.72	4.12	0.613

encompasses only the optimization of regression coefficients; it does not encompass optimization of the choice of descriptors. That is, the regression model is validated only for the specific subset of descriptors obtained from GFA. In contrast, full cross-validation encompasses the entire algorithm, including both the choice of descriptors and the optimization of regression coefficients. For the jackknife “leave-one-out” rule, each full cross-validation step finds the best subset of descriptors for a training set of  $N - 1$  compounds. Here, the full cross-validated  $r^2$  was computed using the predicted values of the missing molecules. The process was repeated until every compound had been left out and predicted once. Cross-validated  $r^2$  was then calculated on the basis of predictions by the models obtained from the remaining compounds in the data set.

## RESULTS AND DISCUSSION

In the present study, 23 molecules were used in the training set (Table 1) to derive QSAR models with the number of

molecular descriptors being not more than four per model. To evaluate the predictive ability of generated QSAR models, a test set of nine molecules with regularly distributed biological activities was used (Table 2). A prerequisite for QSAR study is a congeneric series of molecules, all having the same mechanistic profiles with similar functional properties. Congenericity is a challenging task to define, though it is well-documented that all molecules in a set should have the same molecular framework with structural variation in one or several positions. The molecules used in the study were mostly diaryls or a monoaryl attached to a hydrophobic group. In most of the cases, small alkyl substituents were present on one of the hydrophobic groups, whereas an acidic group was present on the other. The conformational space of the rotatable bonds in the molecule was explored using a random sampling technique in order to obtain sterically accessible conformations within optimum computational time. A conformational search by a random sampling method was performed, using the MSA technique, and lowest-energy conformers were selected for the pharmacophore alignment of the molecules. On successful runs of GFA, different sets of equations were generated by keeping the chain length of equations to four, which were further analyzed statistically to select the best model. As shown in Table 5, three models were selected using a combination of different descriptors.

Model A describes the best system for COX-1 activity; Model B justifies COX-2 activity, whereas Model C gives information about the selectivity index for COX-2 inhibition. The frequent occurrence of AlogP in all of the models and APol in models B and C is clear evidence of the underlying importance of thermodynamic and electronic descriptors for the inhibition of both COX isoforms and COX-2 selectivity for the current series of molecules. AlogP is the thermodynamic descriptor wherein the partition coefficient is calculated using an atom-based approach and represents the hydrophobic requirements of the molecules required to exert an optimum activity profile.<sup>33</sup> AlogP is correlated positively for both COX-2 inhibition and selectivity, whereas it is negatively correlated with COX-1 activity. The large active site of the human COX-2 enzyme being hydrophobic in nature over COX-1, molecules with proper lipophilicity and bulkiness may enhance the enzyme inhibition property as observed in most of the active compounds. This property assumes significance in the present case because of the fact that the conventional NSAIDs possess greater lipophilic character as compared to COX-2-selective inhibitors. This indicates that, when conventional NSAIDs with more lipophilic character become less lipophilic because of increased polarization, COX-2 selectivity increases. Apol, an electronic descriptor, is a sum of atomic polarizabilities related to the distribution of mass and is also proportional to the number of valence electrons in a molecule, as well as how tightly they are bound to their nuclei. The positive correlation of Apol with both COX-2 activity and selectivity is important because this term is unique for the tricyclic class of COX-2 inhibitors due to the presence of nitrogen (in most of the molecules) or sulfur or oxygen in the polycyclic fused central ring. The Apol term in the QSAR models supports the fact that molecules containing unsubstituted nitrogen in the ring are more active than the corresponding substituted analogues.<sup>15</sup> This implicates the possibility of charge transfer and electronic interactions between the ligand and enzyme



**Table 3.** Descriptors Used in the Present Study

sr. no.	descriptor	type	description
1	DIFFV	MSA	difference volume
2	COSV	MSA	common overlap steric volume
3	Fo	MSA	common overlap volume ratio
4	NCOSV	MSA	noncommon overlap steric volume
5	ShapeRMS	MSA	RMS to shape reference
6	SR Vol	MSA	volume of shape reference compound
7	Vm	spatial	molecular volume
8	Area	spatial	molecular surface area
9	Density	spatial	molecular density
10	RadOfGyr	spatial	radius of gyration
11	PMI-mag	spatial	principal moment of inertia X component
12	PMI-X	spatial	principal moment of inertia Y component
13	PMI-Y	spatial	principal moment of inertia Z component
14	PMI-Z	spatial	principal moment of inertia
15	Charge	electronic	sum of partial charges
16	Apol	electronic	sum of atomic polarizabilities
17	Dipole-mag	electronic	dipole moment
18	HOMO	electronic	highest occupied molecular orbital energy
19	LUMO	electronic	lowest unoccupied molecular orbital energy
20	Sr	electronic	super delocalizability
21	Energy	electronic	energy
22	MW	structural	molecular weight
23	RotlBonds	structural	number of rotatable bonds
24	HbondAcc	structural	number of hydrogen bond acceptors
25	HbondDon	structural	number of hydrogen bond donors
26	AlogP	thermodynamic	logarithm of partition coefficient
27	Fh <sub>2</sub> o	thermodynamic	desolvation free energy for water
28	Foct	thermodynamic	desolvation free energy for octanol
29	Hf	thermodynamic	heat of formation
30	molRef	thermodynamic	molar refractivity
31	Kier1	topological	Kier index first order
32	Kier2	topological	Kier index second order
33	Kier3	topological	Kier index third order

**Table 4.** Results of Randomization Tests

confidence level	trials	$r^2_{\text{nonrandom}}$	$r^2_{\text{random}}$ (mean)	SD <sup>a</sup>	SD <sup>b</sup>	$r^2 <^c$	$r^2 >^d$
95%	19	0.775	0.194	4.12	0.194	19	0
98%	49	0.775	0.163	4.23	0.163	49	0

<sup>a</sup> Number of standard deviations of the mean value of  $r^2$  of all random trials to the nonrandom  $r^2$  value. <sup>b</sup> Standard deviation of the  $r^2$  values of all random trials from the mean value of  $r^2$ . <sup>c</sup> Number of  $r^2$  values from random trials that are less than the  $r^2$  value for the nonrandom trial. <sup>d</sup> Number of  $r^2$  values from random trials that are greater than the  $r^2$  value for the nonrandom trial.

responsible for the activity.

**Interpretation of Model A.** When the model for COX-1 inhibition (Model A) was interpreted, observations from the variable usage graph (not shown) indicated that the terms HOMO, AlogP, Vm, and H-bond donor contribute more significantly than all other descriptors used in the generation of QSAR models. An analysis of the statistical performance of the generated QSAR model exhibited moderate internal and external predictivity. Since the predictive  $r^2$  values of various generated QSAR models was similar, their ability to predict and handle training set data was used as the criteria for the selection of the best equation. Model A showed only one outlier for the training set with a greater correlation coefficient, the lowest LOF, and the least possible intervariable correlation comparatively and thus was selected to describe the best model for COX-1 activity. The outlier identified as indomethacin showed large variation with the observed and predicted biological activity. The graph of observed Vs predicted biological activity of the test set molecules (Table 6) for COX-1 inhibition is shown in Figure

1a. The significant statistical interference caused by indomethacin may be due to its structural uniqueness and larger molecular weight, which may tend to increase lipophilicity beyond the ideal requirement of the COX-1 active site in the present series of molecules inhibiting the COX-1 enzyme.

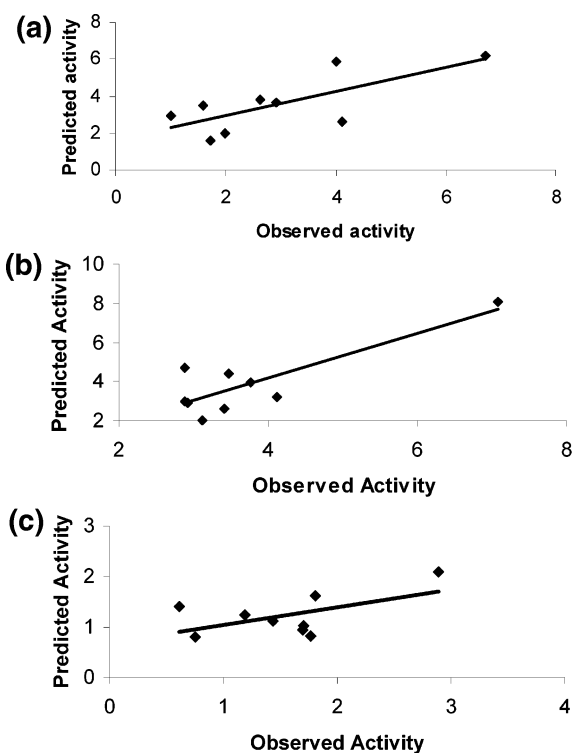
The highest-occupied molecular orbital (HOMO), an electronic parameter, is the highest energy level in the molecule that contains electrons. It is a crucial factor that governs the molecular reactivity and properties. When a molecule acts as an electron-pair donor in bond formation, the electrons are supplied from the molecule's HOMO. How readily this occurs is reflected in the energy of the HOMO. Molecules with a high HOMO are able to donate electrons and hence are relatively more reactive compared to the molecules with low-lying HOMOs. The HOMO measures the nucleophilicity of the molecule. The coefficient of the HOMO is positive, which proposes that, for the activity of COX-1 inhibition, the HOMO energy should be high. In the present series of molecules, compounds having a carboxylic functional group with high HOMO energy (e.g., Flurbiprofen, Ketorolac, Sulindac, Ketoprofen, etc.) indicate that H-bonding interactions between the terminal ionizable functional group of conventional NSAIDs and amino acid residues of the COX-1 enzyme active site are crucial in the ligand–receptor interactions. Furthermore, ion-pair interactions between ionizable functional groups of inhibitor molecules and signature motif amino acid residues like Arg120 of COX-1 enzyme form a salt bridge and serve as a key recognition element in the ligand–receptor interactions.<sup>34</sup> This evidence supports the importance of a positively correlated HOMO descriptor in the QSAR equation in

**Table 5.** Summary of the Best QSAR Equations Selected from GFA Models

model	equation	LOF	F value	$r^2$	$r^2_{cv}$	$r^2_{BS}$	$r^2_{pred}$
Model A	COX-1 BA = $-12.358 + 0.720(\text{HOMO}) - 0.424(\text{AlogP}) + 0.031(\text{Vm}) + 1.140(\text{HBondDon})$	0.304	59.625	0.775	0.710	0.776	0.581
Model B	COX-2 BA = $-5.033 + 0.027(\text{COSV}) + 0.624(\text{Dipole-mag}) + 0.31(\text{Apol}) + 0.484(\text{AlogP})$	1.801	42.092	0.766	0.631	0.769	0.532
Model C	SI = $1.823 - 0.241(\text{HBondAcc}) + 0.095(\text{AlogP}) + 0.108(\text{Apol}) - 0.002(\text{Hf})$	0.160	40.329	0.776	0.685	0.779	0.550

**Table 6.** GFA Predicted Activity Values Using Generated QSAR Models

test set molecules	Model A			Model B			Model C		
	actual COX-1	predicted COX-1	residual	actual COX-2	predicted COX-2	residual	actual SI	predicted SI	residual
Tiracoxib	4.000	5.831	-1.831	7.070	8.063	-0.993	1.767	0.826	0.941
Sulindac	1.720	1.575	0.145	2.920	2.901	0.019	1.697	0.945	0.752
L-745337	1.000	2.928	-1.928	2.890	4.715	-1.825	2.890	2.088	0.802
Flubiprofen	4.120	2.585	1.535	3.110	1.967	1.143	0.754	0.808	-0.054
Celecoxib	2.920	3.636	-0.716	3.470	4.415	-0.945	1.188	1.240	-0.052
Nimesulide	2.000	1.974	0.026	3.410	2.581	0.829	1.705	1.030	0.675
Mefenamate	1.600	3.522	-1.922	2.890	2.949	-0.059	1.806	1.616	0.190
Piroxicam	2.620	3.828	-1.208	3.770	3.960	-0.19	1.438	1.125	0.313
Ketorolac	6.720	6.192	0.528	4.120	3.163	0.957	0.613	1.409	-0.796

**Figure 1.** (a) A graph of observed versus predicted activities of test set molecules for COX-1 inhibition using Model A. (b) A graph of observed versus predicted activities of test set molecules for COX-2 inhibition using Model B. (c) A graph of observed versus predicted activities of test set molecules for the selectivity index using Model C.

governing the potency of COX-1 inhibitors.

Vm, a spatial descriptor, defines the molecular volume of the ligand inside the contact surface with the receptor during ligand–receptor interactions. Molecular volume is related to the binding and transport of a drug molecule to exert its therapeutic potency. This descriptor represents the importance of the size and shape of the molecule to bind tightly with the enzyme during ligand–receptor interactions. A positively correlated Vm indicated that the molecules under study should necessarily possess a volume such as that of the shape

reference molecule (Tenoxicam) to bind effectively with the receptor. This is also supported by the geometry of most of the COX-1 inhibitors existing in a planar conformation with respect to the pocket of the COX-1 enzyme. Phenazone with less molecular volume compared to the shape reference compound (Tenoxicam) showed less biological activity, whereas sulindac with large molecular volume showed increased COX-1 inhibition. Some of the molecules in the present study having a large molar volume, although having less inhibitory activity against COX-1, exceptionally proved to possess a moderate degree of COX-2 inhibition.

The H-bond donor is positively correlated to the biological activity for COX-1 inhibition and indicates that the presence of a H-bond donor group(s) in the molecule favors the retention of the activity. The bridging  $-N-$  of two benzene rings of diclofenac has a hydrogen donor group which should be unsubstituted for better activity against COX-1 or if substituted should contain H-bond donor groups. For example, the methyl-substituted  $-N-$  of pyrrole in zomiperac is less potent than that of diclofenac.

**Interpretation of Model B.** Model B best describes COX-2 activity as confirmed by validation of the model judging internal and external predictivity, variable terms, the LOF value, and other statistical terms like the  $F$  value. The variable terms in the equation show low correlation among themselves, indicating a lesser probability of chance correlation. As indicated by the variable usage graph, the generation of the equation (Model B) for COX-2 inhibitory activity was dominated by repeated use of the AlogP, COSV, Dipole-mag, and Apol features.

COSV is a molecular shape analysis parameter which, when appearing in the generated QSAR model, clearly suggests the significance of common volume between the shape reference (DuP-697) and other analogues. Because the shape reference molecule is the one with the highest biological activity and COSV is positively correlated, molecules that are structurally/conformationally similar to it are expected to exhibit greater activity. This also suggests that, for a molecule to be COX-2-active, the structural volume of the molecule must be equal to the volume of the

reference molecule. This has been well-supported as the volume of the COX-2-active site is approximately 20–25% larger than that of COX-1, because the presence of a smaller amino acid in position 523 in COX-2 (valine in COX-2; isoleucine in COX-1) induces a conformational change, thereby forming an additional hydrophobic secondary internal pocket protruding off the primary binding site which is absent in COX-1.<sup>34,35</sup> Consequently, the total volume of the primary binding site of COX-2 and its associated secondary pocket (394 Å<sup>3</sup>) is about 20–25% larger than that of the COX-1 binding site (316 Å<sup>3</sup>). Though the molecules lack traditional requisite functional groups, they are capable of occupying a larger area (84.18% by the most active molecule) in the active site probably because of their bulkiness (331.70 Å<sup>3</sup> for the most active) and making favorable interactions with active site residues and, hence, are active.

The presence of COSV also indicates the contribution of conformational rigidity and proper orientation of the two aromatic rings attached to the central nucleus of the molecule. As evidenced from the crystallographic data of two COX isoforms, the (COX-1)Phe → (COX-2)Leu substitution at position 503 is thought to increase the flexibility of COX-2 in this region of the binding site.<sup>36</sup> Bernard et al. have described that the attachment of polycyclic rings increases the bulkiness (steric), and an increase in the hydrophobic character of the inhibitors enhances the enzyme inhibition property.<sup>37</sup> This may be due to the attachment of polycyclic rings to the central nucleus, which may additionally offer proper rigidity and in turn allow the two aromatic rings to have proper conformation, so as to occupy a larger area in the active site of the enzyme.

The electronic attributes in drug receptor interaction are represented by the dipole moment. Different substituents in a series of drugs in an electrostatic field directly interact with the receptor via charge–dipole, dipole–dipole, dipole–induced-dipole, and induced-dipole–induced-dipole interactions. The dipole moment is the quantitative measurement of the separation of charge and is useful in describing the direct drug receptor interaction through noncovalent bonding. The dipole moment of the molecule should be high for a compound to be COX-2-active, and electronic effects exerted by dipole moments are important for the binding of a drug to the COX-2 enzyme. It has been well-studied that the presence of a water molecule in the binding cavity introduces intermolecular electrostatic interactions with the negatively charged oxygen atom of the water molecule, which favors interactions with halogens.<sup>38</sup> These kinds of interactions are common in COX-2 enzyme inhibitors, particularly in the case of tricyclic inhibitors. The primary and secondary active sites of the COX-2 enzyme are lined by amino acid residues that are capable of having electrostatic interactions with appropriate functional groups present in the inhibitors, for example, (a) His90, Gln192, and Tyr355 (which control the access of ligands into the secondary pocket by a hydrogen-bonding network);<sup>39</sup> (b) Tyr385, Ser530, Arg120, and recently Arg513 in the primary active site.<sup>40</sup> Recent molecular modeling studies reveal that the water molecules present near the mouth of the active site play a major role in the remodeling of the hydrogen-bonding network involving Arg120 and Glu524, which is necessary for time-dependent inhibition of the enzyme. In the present study, the contribution of the dipole moment is mainly from aromatic rings and its substituents

like fluoro and heterocyclic nitrogen of the central ring. The SAR of molecules under study revealed that molecules with an unsubstituted heterocyclic nitrogen in the central ring and fluoro-substituted aromatic rings have retained the enzyme inhibition profile. It may be due to participation of the –H– of the ring nitrogen in the hydrogen bond formation with the water molecules, or the functional groups present on the aromatic rings may have electrostatic interactions with the active site residues as mentioned above.

However, the major obstacle in 3D-QSAR studies lies with the “congeners” which misfit the final equation and were termed as outliers. The predictive ability of the equation derived for COX-2 inhibition was significantly increased ( $r^2_{\text{pred}} = 0.532$ ) when Model B showed two outliers as being indomethacin and meloxicam. Figure 1b shows a graph of actual and predicted activities of test set molecules (Table 6) for COX-2 inhibition obtained from Model B. The reasons for poor prediction may be their structural uniqueness and insignificant mathematical value in defining the biological activity. In addition, the occurrence of indomethacin as an outlier in both Model A and Model B may be because of disfavored orientation of the p-chloro benzoyl moiety linked with indolyl nitrogen. However, the present series of diverse sets of molecules showed significant statistical interference, which may be due to a lesser accuracy of the biological values. In the human whole blood assay from which activity values are used to derive correlation, celecoxib is just 3.5 times more selective for COX-2 over COX-1. In contrast, when recombinant human COX-1 and COX-2 from broken insect cells is used, celecoxib is between 155- and 3200-fold more selective in WBA and WHMA and is not modeled well in these assays. The IC<sub>50</sub> value of ketorolac for COX-1 is extremely lower than those of the other compounds used in this study, and it could be possible that it is not modeled well.

**Interpretation of Model C.** The selectivity index model (Model C) resulted in high precision as indicated by an increase in internal as well as external consistency, a higher F value, and a lower LOF value. The graph of observed Vs predicted biological activity of the test set molecules (Table 6) for the COX-2/COX-1 ratio is shown in Figure 1c. Observations from the varied selectivity index differences as predicted by GFA may be due to the fact that highly rigid structures such as etodolac reduce the flexibility of the molecule, restricting favorable drug–receptor interactions.

An interesting trend was observed with the thermodynamic descriptor AlogP while developing Model C to obtain optimum COX-2 selectivity, which was found to contribute negatively in Model A and positively in Model B. This signifies that the incorporation of optimal lipophilic characters in the molecules significantly modulates the selectivity trend. Other descriptors found to significantly contribute toward the selectivity trend are thermodynamic (Hf), structural (HBondAcc), and electronic (Apol) features.

Hf (heat of formation) is a thermodynamic parameter and accounts for the chemical stability of the molecule. The negative coefficient of this term in Model C explains that lower the value, the better the activity, suggesting that the biological activity with respect to COX-2 selectivity is directly dependent upon the chemical stability of the molecules in biochemical systems.



The hydrogen-bond acceptor is a structural parameter and shows negative correlation as against the case of Model A where the H-bond donor descriptor partially shares COX-1 inhibition. This indicates that, for a compound to be optimally COX-2-selective, it should have reasonable hydrogen-bond acceptors. This is true for highly selective compounds like nimesulide, rofecoxib, valdecoxib, and so forth, which have maximum hydrogen-bond acceptors relative to the nonselective NSAIDs like ibuprofen, indomethacin, and so forth. This highest degree of COX-2 inhibition may lead to initiating untoward cardiovascular effects, resulting in the withdrawal of these drugs from the market.<sup>12</sup> It is also proved from docking studies for COX-2-selective inhibitors that there exist one to three H bonds with the net total being at least six, whereas in the case of COX-1-selective NSAIDs, there are only one to three H-bond interactions with the net total being that at least four are involved.<sup>41</sup> Thus, the H-bond accepting and donating ability of a molecule defines the selectivity index for the two COX isoforms. Previously, it was found that COX-2 selectivity could only be achieved by the use of H-bonding pharmacophores such as  $\text{SO}_2\text{CH}_3$ ,  $\text{SO}_2\text{NH}_2$ ,  $\text{NH}\text{SO}_2\text{CH}_3$ , and so forth, which satisfies the secondary pocket of COX-2 and inhibits COX-2 efficiently.<sup>41</sup> However, Bernard et al.<sup>37</sup> and Raichurkar and Kulkarni<sup>15</sup> showed that the sulfonyl group is not a structural requisite for COX-2 inhibition. Thus, replacing the sulfonyl group with simple and small substituents like  $-\text{OCH}_3$ ,  $-\text{SCH}_3$ ,  $-\text{OCH}_2\text{CH}_3$ ,  $-\text{NHNH}_2$ ,  $-\text{C}=\text{N}-\text{CH}_2\text{CH}_3$ , and so forth may reasonably modulate COX-2 activity to achieve optimum selectivity in order to avoid cardiovascular side effects. However, considering the diversity of the molecules used in this 3D-QSAR study, the results obtained provide useful information regarding the factors responsible for the activity and selectivity of NSAIDs for cyclooxygenase isoenzymes.

### CONCLUSIONS

A 3D-QSAR analysis on a structurally diverse set of known NSAIDs of clinical practice with COX-1 and COX-2 inhibitory activity and their selectivity for COX-2 inhibition was performed to find factors contributing to the activity and selectivity. GFA, a robust statistical technique, handled the physicochemical descriptors effectively. The generated models were analyzed and validated for their statistical significance and external prediction power. A randomization test and intervariable correlation matrix were used to check the possibility of "chance correlation" for the generated models. The variables in the equation reveal that thermodynamic, electronic, structural, and molecular shape analysis descriptors contribute significantly for COX-2 potency and optimum selectivity. The evaluation and comparison of QSAR models generated for achieving optimum COX-2 selectivity and potency provide understanding that the inhibition of the COX-2 enzyme by this diverse set of molecules may be noncovalent in nature, and this leads to few significant conclusions: (1) The presence of H-bond acceptors and donors potentiates COX-2 selectivity and activity. Thus, restricting them to a reasonable level minimizes H-bonding interactions and obtains an optimum COX-2 selectivity index thereby preventing cardiovascular side effects. (2) The number of valence electrons in the molecule such as heterocyclic N, S, and O brings charge-transfer electrostatic interactions with precise chemical

stability in the biochemical system and crucially governs the COX-2 activity and selectivity. (3) The modulation of COX-2 selectivity can be best achieved by increasing the flexibility of the molecule due to the presence of a higher number of rotatable bonds. (4) Since more lipophilic characters tend to favor COX-1 selectivity and a less lipophilic nature of the molecule enhances COX-2 selectivity, a molecule should be tuned in a way so as to cover up a precise hydrophilic–lipophilic balance. (5) Maintaining the bulkiness on the molecule and providing specific conformation to the molecule can also achieve an optimum selectivity index.

In summary, results from the analysis of 3D-QSAR models connote to the rationalization of the COX-1 and COX-2 binding profiles, leading to the identification of structural and physicochemical requirements for enhancing reasonable affinity toward COX-2 in a qualitative and quantitative way.

Moreover, the awareness and understanding of the descriptors involved in both the affinity and selectivity properties of these compounds could provide a great opportunity to the ligand structures with appropriate features and how they affect the biological data upon binding to COX-1 and COX-2. It is clear that SAR information extracted from this kind of analysis could provide guidelines for the drug design process. As a consequence, the outcome of this study could be kept as a guide for the further development of safer COX-2 inhibitors with high affinity and optimum selectivity properties toward the target of interest.

### ACKNOWLEDGMENT

The authors thank University Grants Commission (UGC) for the sanction of a Departmental Research Support (DRS) project to Poona College of Pharmacy under its Special Assistance Program (SAP) and Dr. S.S. Kadam for encouragement.

### REFERENCES AND NOTES

- (1) Insel, P. A. Analgesic–Antipyretic and Antiinflammatory Agents and Drugs Employed in the Treatment of Gout. In *The Pharmacological Basis of Therapeutics*, 9th ed.; Hardman, J., Limbird, L., Molinoff, P., Ruddon, R., Goodman, A., Eds.; McGraw Hill: New York, 1996; pp 617–657.
- (2) Vane, J. R. Inhibition of Prostaglandin Synthesis as a Mechanism of Action for Aspirin-Like Drugs. *Nature New Biol.* **1971**, *231*, 232–235.
- (3) Marnett, L. J.; Kalutkar, A. S. Cyclooxygenase 2 Inhibitors: Discovery, Selectivity and the Future. *Trends Pharm. Sci.* **1999**, *20*, 465–469.
- (4) Allison, M. C.; Howatson, A. G.; Torrance, C. J.; Lee, F. D.; Russel, R. I. Gastrointestinal Damage Associated with the Use of Nonsteroidal Antiinflammatory Drugs. *New Engl. J. Med.* **1992**, *327*, 749–754.
- (5) Garell, S.; Matarese, R. A. Renal Effects of Prostaglandins and Clinical Adverse Effects of Non-Steroidal Anti-Inflammatory Agents. *Medicine* **1984**, *63*, 165–181.
- (6) Warner, T. D.; Giulino, F.; Vojnovic, I.; Bukasa, A.; Mitchel, J. A.; Vane, J. R. Nonsteroid Drug Selectivities for Cyclooxygenase-1 Rather Than Cyclooxygenase-2 Are Associated with Human Gastrointestinal Toxicity: A Full in Vitro Analysis. *Proc. Natl. Acad. Sci. U.S.A.* **1999**, *96*, 7563–7568.
- (7) Penning, T. D.; Talley, J. J.; Bertenshaw, S. R.; Carter, J. S.; Collins, P. W.; Docter, S.; Graneto, M. J.; Lee, L. F.; Malecha, J. W.; Miyashiro, J. M.; Rogers, R. S.; Rogier, D. J.; Yu, S. S.; Anderson, G. D.; Burton, E. G.; Cogburn, J. N.; Gregory, S. A.; Koboldt, C. M.; Perkins, W. E.; Seibert, K.; Veenhuizen, A. W.; Zhang, Y. Y.; Isakson, P. C. Synthesis and Biological Evaluation of the 1,5-Diarylpyrazole Class of Cyclooxygenase-2 Inhibitors: Identification of 4-[5-(4-Methylphenyl)-3-(trifluoromethyl)-1H-pyrazol-1-yl] Benzene Sulfonamide (SC-58635, Celecoxib). *J. Med. Chem.* **1997**, *40*, 1347–1365.
- (8) Prasit, P.; Wang, Z.; Brideau, C.; Chan, C. C.; Charleson, S.; Cromlish, W.; Ethier, D.; Evans, J. F.; Ford-Hutchinson, A. W.; Gauthier, J. Y.;



- Gordon, R.; Guay, J.; Gresser, M.; Kargman, S.; Kennedy, B.; Leblanc, Y.; Leger, S.; Mancini, J.; O'Neill, G. P.; Ouellet, M.; Percival, M. D.; Perrier, H.; Riendeau, D.; Rodger, I.; Zamboni, R.; Boyce, S.; Rupniak, N.; Forrest, M.; Visco, D.; Patrick, D. The Discovery of Rofecoxib, [MK 966, Vioxx, 4-(4'-Methylsulfonylphenyl)-3-phenyl-2(5H)-furanone], an Orally Active Cyclooxygenase-2-Inhibitor. *Bioorg. Med. Chem. Lett.* **1999**, 9, 1773–1778.
- (9) Talley, J. J.; Brown, D. L.; Carter, J. S.; Graneto, M. J.; Koboldt, C. M.; Masferrer, J. L.; Perkins, W. E.; Rogers, R. S.; Shaffer, A. F.; Zhang, Y. Y.; Zweifel, B. S.; Seibert, K. 4-[5-Methyl-3-phenylisoxazol-4-yl]-benzenesulfonamide, Valdecoxib: A Potent and Selective Inhibitor of COX-2. *J. Med. Chem.* **2000**, 43, 775–777.
- (10) Talley, J. J.; Bertenshaw, S. R.; Brown, D. L.; Carter, J. S.; Graneto, M. J.; Kellogg, M. S.; Koboldt, C. M.; Yuan, J.; Zhang, Y. Y.; Seibert, K. N-[[[5-Methyl-3-phenylisoxazol-4-yl]-phenyl] Sulfonyl] Propanamide, Sodium Salt, Parecoxib Sodium: A Potent and Selective Inhibitor of COX-2 for Parenteral Administration. *J. Med. Chem.* **2000**, 43, 1661–1663.
- (11) Riendeau, D.; Percival, M. D.; Brideau, C.; Charleson, S.; Dube, D.; Ethier, D.; Falgoutet, J. P.; Friesen, R. W.; Gordon, R.; Greig, G.; Guay, J.; Mancini, J.; Ouellet, M.; Wong, E.; Xu, L.; Boyce, S.; Visco, D.; Girard, Y.; Prasit, P.; Zamboni, R.; Rodger, I. W.; Gresser, M.; Ford-Hutchinson, A. W.; Young, R. N.; Chan, C.-C. Etoricoxib (MK-0663): Preclinical Profile and Comparison with Other Agents That Selectively Inhibit Cyclooxygenase-2. *J. Pharmacol. Exp. Ther.* **2002**, 296, 558–566.
- (12) Solomon, D. H.; Schneeweiss, S.; Glynn, R. N.; Kiyota, Y.; Levin, R.; Mogun, H.; Avorn, J. Relationship between Selective Cyclooxygenase-2 Inhibitors and Acute Myocardial Infarction in Older Adults. *Circulation* **2004**, 109, 2068–2073.
- (13) Desiraju, G. R.; Gopalakrishnan, B.; Jetty, R. K. R.; Raveendra, D.; Sarma, J. A. R. P.; Subramanya, H. S. Three-Dimensional Quantitative Structural Activity Relationship (3D-QSAR) Studies of Some 1,5-Diarylpyrazoles: Analogue Based Design of Selective Cyclooxygenase-2 Inhibitors. *Molecules* **2000**, 5, 945–955.
- (14) Chavatte, P.; Yous, S.; Marot, C.; Baurin, N.; Lesieur, D. Three-Dimensional Quantitative Structure-Activity Relationships of Cyclooxygenase-2 (COX-2) Inhibitors: A Comparative Molecular Field Analysis. *J. Med. Chem.* **2001**, 44, 3223–3230.
- (15) Raichurkar, A. V.; Kulkarni, V. M. 3D-QSAR of Cyclooxygenase-2 Inhibitors by Genetic Function Approximation. *Int. Electron. J. Mol. Des.* **2003**, 2, 242–261.
- (16) Luong, C.; Miller, A.; Barnett, J.; Chow, J.; Ramesha, C.; Browner, M. F. Flexibility of the NSAID Binding Site in the Structure of Human Cyclooxygenase-2. *Nat. Struct. Biol.* **1996**, 3, 927–933.
- (17) Gokhale, V. M.; Kulkarni, V. M. Understanding the Antifungal Activity of Terbinafine Analogues Using Quantitative Structure–Activity Relationship (QSAR) Models. *Bioorg. Med. Chem.* **2000**, 8, 2487–2499.
- (18) Karki, R. G.; Kulkarni, V. M. Three-Dimensional Quantitative Structure Activity Relationship (3D-QSAR) of 3-Aryloxazolidin-2-one Antibacterials. *Bioorg. Med. Chem.* **2001**, 9, 3153–3160.
- (19) Makhija, M. T.; Kulkarni, V. M. QSAR of HIV-1 Integrase Inhibitors by Genetic Function Approximation Method. *Bioorg. Med. Chem.* **2002**, 10, 1483–1497.
- (20) Vadlamudi, S. M.; Kulkarni, V. M. 3D-QSAR of Protein Tyrosine Phosphatase 1B Inhibitors by Genetic Function Approximation. *Int. Electron. J. Mol. Des.* **2004**, 3, 586–609.
- (21) Kharkar, P. S.; Desai, B.; Varu, B.; Loria, R.; Naliyapara, Y.; Gaveria, H.; Shah, A.; Kulkarni, V. M. Three-Dimensional Quantitative Structure Activity Relationship of 1,4-Dihydropyridines as Antitubercular Agents. *J. Med. Chem.* **2002**, 45, 4858–4867.
- (22) Rogers, D. G/SPLINES: A Hybrid of Friedman's Multivariate Adaptive Regression Splines (MARS) Algorithm with Holland's Genetic Algorithm. In *Proceedings of the Fourth International Conference on Genetic Algorithms*, San Diego, CA, 1991; Belew, R. K., Booker, L. B., Eds.; Morgan Kaufmann Publishers Inc.: San Mateo, CA, 1991.
- (23) Rogers, D.; Hopfinger, A. J. Applications of Genetic Function Approximation to Quantitative Structure–Activity Relationships and Quantitative Structure–Property Relationships. *J. Chem. Inf. Comput. Sci.* **1994**, 34, 854.
- (24) Cerius2, version 3.5; Molecular Simulations Inc.: San Diego, CA.
- (25) Venkatarangan, P.; Hopfinger, A. J. Prediction of Ligand–Receptor Binding Thermodynamics by Free Energy Force Field 3D-QSAR Analysis: Application to a Set of Glucose Analogue Inhibitors of Glycogen Phosphorylase. *J. Med. Chem.* **1999**, 42, 2169–2179.
- (26) Tokarski, J. S.; Hopfinger, A. J. Prediction of Ligand–Receptor Binding Thermodynamics by Free Energy Force Field 3D-QSAR Analysis: Application to a Set of Peptidomimetic Renin Inhibitors. *J. Chem. Inf. Comput. Sci.* **1997**, 37, 792–811.
- (27) Hann, M.; Rogers, D. Receptor Surface Models. 2. Application to QSAR Studies. *J. Med. Chem.* **1995**, 38, 2091–2102.
- (28) Fan, Y.; Shi, L. M.; Kohn, K. W.; Pommier, Y.; Weinstein, J. N. Quantitative Structure–Antitumor Activity Relationship of Camptothecin Analogues: Cluster Analysis and Genetic Algorithm Based Studies. *J. Med. Chem.* **2001**, 44, 3254–3263.
- (29) Rappe, A. K.; Goddard, W. A., III. Charge Equilibration for Molecular Dynamics Simulations. *J. Phys. Chem.* **1991**, 95, 3358–3363.
- (30) Hopfinger, A. J. A Quantitative Structure Activity Relationship: Investigation of Dihydrofolate Reductase Inhibition by Baker Triazines Based Upon Molecular Shape Analysis. *J. Am. Chem. Soc.* **1980**, 102, 7196–7206.
- (31) Waller, C. L.; Opera, T. I.; Giolitti, A.; Marshall, G. R. Three-Dimensional QSAR of Human Immunodeficiency Virus (1) Protease Inhibitors. 1. A CoMFA Study Employing Experimentally Determined Alignment Rules. *J. Med. Chem.* **1993**, 36, 4152–4160.
- (32) Cramer, R. D., III.; Bunce, J. D.; Patterson, D. E. Cross-Validation, Bootstrapping and Partial Least Squares Compared With Multiple Regressions in Conventional QSAR Studies. *Quant. Struct.-Act. Relat.* **1988**, 7, 18–25.
- (33) Viswanathan, V. M.; Goshe, A. K.; Revanker, G. R.; Robbins, R. K. Atomic Physicochemical Parameters for Three Dimensional Structure Directed Quantitative Structure–Activity Relationships. 4. Additional Parameters for Hydrophobic and Dispersive Interactions and Their Application for an Automated Superposition of Certain Naturally Occurring Nucleoside Antibiotics. *J. Chem. Inf. Comput. Sci.* **1989**, 29, 163–172.
- (34) Kurumbail, R. G.; Stevens, A. M.; Gierse, J. K.; McDonald, J. J.; Stegeman, R. A.; Pak, J. Y.; Gildehaus, D. J.; Miyashiro, M.; Penning, T. D.; Seibert, K.; Isakson, P. C.; Stallings, W. C. Structural Basis for Selective Inhibition of Cyclooxygenase-2 by Antiinflammatory Agents. *Nature* **1996**, 384, 644–648.
- (35) Gierse, J. K.; McDonald, J. J.; Hauser, S. D.; Rangwala, S. H.; Koboldt, C. M.; Seibert, K. A Single Amino Acid Difference Between Cyclooxygenase-1 (COX-1) and -2 (COX-2) Reverses the Selectivity of COX-2 Specific Inhibitors. *J. Biol. Chem.* **1996**, 271, 15810–15814.
- (36) Marnett, L. J.; Kalgutkar, A. S. Design of Selective Inhibitors of Cyclooxygenase-2 as Nonulcerogenic Anti-Inflammatory Agents. *Curr. Opin. Chem. Biol.* **1998**, 2, 482–490.
- (37) Bernard, P.; Charles, T.; Philippe, P.; Jacqueline, B.; Guillaume, De, N. 1,3-Diaryl–4,5,6,7-tetrahydro-2H-isoindole Derivatives. A New Series of Potent and Selective COX-2 Inhibitors in which a Sulfonyl Group Is Not a Structural Requisite. *J. Med. Chem.* **2000**, 43, 4582–4593.
- (38) Plouffe, M. L.; Jorgensen, W. L. Analysis of Binding Affinities for Celecoxib Analogues with COX-1 and COX-2 from Combined Docking and Monte Carlo Simulations and Insight into the COX-2/COX-1 Selectivity. *J. Am. Chem. Soc.* **2000**, 122, 9455–9466.
- (39) Llorens, O.; Perez, J. J.; Palomer, A.; Mauleon, D. Structural Basis of The Dynamic Mechanism of Ligand Binding to Cyclooxygenase. *Bioorg. Med. Chem. Lett.* **1999**, 9, 2779–2784.
- (40) Habbe, A. G.; Praveen Rao, P. N.; Knaus, E. E. Design and Synthesis of Celecoxib and Rofecoxib Analogues as Selective Cyclooxygenase-2 (COX-2) Inhibitors: Replacement of Sulfonamide and Methanesulfonyl Pharmacophore by an Azido Bioisostere. *J. Med. Chem.* **2001**, 44, 3039–3042.
- (41) Akaho, E.; Fujikawa, C.; Runion, H. I.; Hill, C. R.; Nakano, H. J. A Study on Binding Modes of Nonsteroidal Anti-Inflammatory Drugs to COX-1 and COX-2 as Obtained by Dock4.0. *J. Chem. Software* **1999**, 5, 1–14.

CI6004367